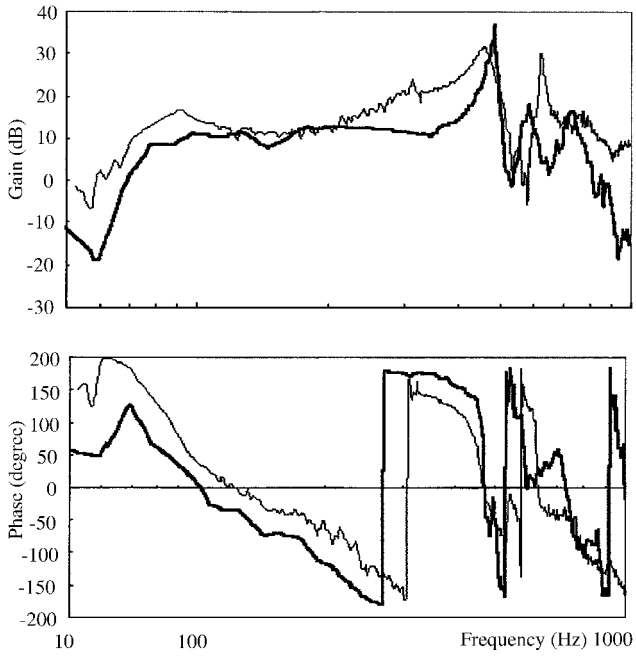

Fig. 3 Transfer function of a rotational accelerometer based on a spatial filter (——) and uniform sensor (——) design.

This experimental result clearly verifies the possibility of enhancing the bandwidth of a rotational acceleration rate sensor by adopting a concept of spatial filters.

Conclusions

The concept and design freedom introduced by adopting spatial filters to second-order partial differential equation systems have been successfully verified by an one-dimensional clamped-free shaft-based rotational acceleration rate sensor. It was shown that spatial filters can introduce a no-phase delay low-pass filter by offering a weighting function with the prechosen surface electrode, and the introduction of this odd function brings a differentiation to the transfer function. The method of imaging was introduced to extend the spatial filter application area from a finite structure to an infinite domain, that is, spatial filters can now be placed near or even at the boundaries. Benefits associated with adopting spatial filters to point sensors successfully demonstrate theoretically as well as experimentally the advantages of the newly developed rotational acceleration rate sensor. In summary, expanding the bandwidth of rotational acceleration rate sensors by using newly developed finite domain spatial filters has been successfully verified both theoretically and experimentally.

References

[1]Miller, D. W., Collins, S. A., and Peltzman, S. P., "Development of Spatially Convolving Sensors for Structural Control Applications," *Proceedings of the AIAA/ASME/ASCE/AHS Structures, Structural Dynamics, and Materials Conference*, edited by B. Prasad, Pt. 4, AIAA, Washington, DC, 1990, pp. 2283–2297.

[2]Meirovitch, L., *Element of Vibration*, McGraw–Hill, New York, 1986, pp. 269, 270, 290–296.

[3]Cady, W. G., *Piezoelectricity*, Vol. 1, McGraw–Hill, New York, 1946, pp. 1–8.

[4]Lee, C. K., "Theory of Laminated Piezoelectric Plates for the Design of Distributed Sensors/Actuators: Part I. Governing Equations and Reciprocal Relationships," *Journal of the Acoustical Society of America*, Vol. 87, No. 3, 1990, pp. 1144–1158.

[5]Hsu, Y. H., and Lee, C. K., "Targeted Origin Placement for the Autonomous Gain-Phase Tailoring of Piezoelectric Sensors," *Smart Materials and Structures*, Vol. 11, No. 3, 2002, pp. 444–458.

[6]Oppenheim, A. V., and Schafer, R. W., *Signal and System*, Prentice–Hall, Upper Saddle River, NJ, 1999, pp. 655–692.

[7]Graff, K. F., *Wave Motion in Elastic Solids*, Dover, New York, 1975, pp. 80–82.

A. Berman
Associate Editor

Assessment of Delamination Fracture Load of Stringer Stiffened Composite Panel

R. Ramesh Kumar,* K. S. Praveen,†
and G. Venkateswara Rao‡
Vikram Sarabhai Space Center,
Thiruvananthapuram 695 022, India

Introduction

STRUCTURAL efficiency is an important aspect in the design of weight-conscious and cost-effective aerospace structures. This can be accomplished in many instances as in the case of stiffness-based design by increasing the stiffness through the use of stringers in the form of hat stiffeners. Efficient use of such composite panels requires that the panels be designed to operate at loads several times their initial buckling load. The composite stiffened panels are normally fabricated by cocuring the skin and stiffener or by bonding the precured stiffener to the skin. Under compressive loading it might fail either by delamination of stringer from the base panel, buckling, or delamination followed by buckling once its compression strength is higher than critical buckling load. The most common failure mode reported in the literature is separation of the stiffener from base panel as a delamination mode of failure.[1–6] However, the effect of this delamination on the failure load of the structure requires major research, and few reports are available in the literature.

In the present work failure is defined as an onset of delamination fracture resulting in separation of the stringer from the panel. One can conclude that for a stringer stiffened panel the most commonly observed failure mode under compressive loading is the delamination fracture. Once a delamination is present, the state of the art is to assess strain energy release rate G and compare it with its critical value Gc to evaluate the margin of safety. So it is essential to assess first the critical buckling load and then the possible damage caused by delamination, and only then can one estimate the margin of safety of the structure accurately. But as of today the aspect of "when a delamination analysis is to be considered" is not fully established in the literature.

The aim of the present study is first to predict the delamination fracture load of a compressively loaded stringer stiffened composite panel based on the strain energy release rate approach and then compare the fracture load thus obtained with both the test data for the failure load and the critical buckling load to assess the integrity of the structure. Finite element analyses are carried out to compare the strains determined from the geometric nonlinear analysis with test data to determine the critical buckling load and the delamination fracture load.

Description of the Test Panel

A composite panel of size 400×750 mm with four hat-type stringer stiffeners cocured with the skin (panel) on one side of the panel is shown in Fig. 1. The top and bottom part of the panel are locally reinforced over length of 50 mm and bolted to an aluminum T-channel section as shown in Fig. 1, which can go through the slit provided in the test setup. The top of the panel is immovable with the test fixture, whereas the bottom is movable in the vertical direction. The structure is made up of M55J/M18 carbon-epoxy prepreg.

Received 21 June 2001; revision received 3 September 2002; accepted for publication 3 September 2002.

*Engineer, Structural Engineering Group.
†Graduate Student; currently Senior Development Engineer, Ashok Leyland, Technical Centre, Chennai 600 101, India.
‡Group Director, Structural Engineering Group.

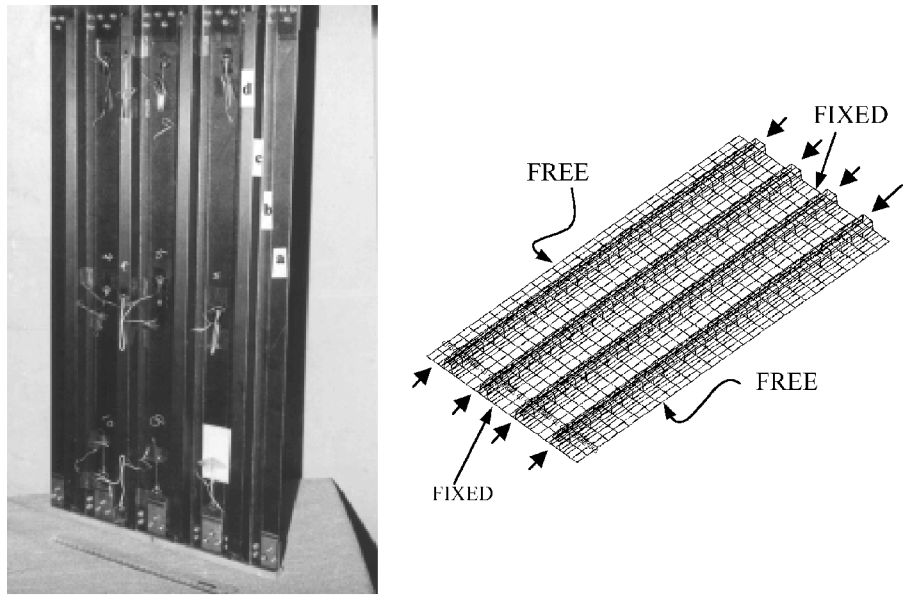

Fig. 1 Details of stringer stiffened (hat-type) composite panel: a) base panel, [30 deg/−30 deg/30 deg/−30 deg/60 deg/−60 deg/−60 deg/60 deg/−30 deg/30 deg/−30 deg/30 deg], 12 layers; b) base of the hat stiffener, [45 deg/−45 deg/−45 deg/45 deg/−45 deg/45 deg/45 deg/−45 deg/30 deg/−30 deg/30 deg/−30 deg/60 deg/−60 deg/−60 deg/60 deg/−30 deg/30 deg/−30 deg/30 deg], 20 layers; c) web of the stiffener, [45 deg/−45 deg/−45 deg/45 deg/−45 deg/45 deg/45 deg/ −45 deg], 8 layers; and d) flange of the hat stiffener, [45 deg/−45 deg/−45 deg/45 deg/−45 deg/45 deg/45 deg/−45 deg/0 deg/0 deg], 10 layers.

The material properties of the unidirectional laminate are given in Ref. 7. Typically, moduli of the unidirectional laminate along and across the fiber are 294.3 and 5.96 GPa, respectively, Poisson's ratio of 0.346, and shear modulus of 4.90 GPa. The details of the layup sequence of the skin and stiffeners are given in Fig. 1. Each layer in a laminate is 0.1 mm thick.

Methodology

Initially, both static and buckling analyses are carried out to ensure that compressive strength capability of the panel is much above the critical buckling load. The compressive failure load evaluated using the Tsai–Wu criterion is compared with the critical buckling load. If the critical buckling load is less than the compressive failure load, then the structure can fail by buckling or by delamination, and hence delamination analysis is required to assess the fracture load.

Testing

The testing was done in INSTRON machine. The compressive load was applied at the rate of 500 kg/min, and the strains were measured at various locations along the length of the panel. The load at which delaminationing occurred was also noted. Delamination fracture occurred at 46.75 kN for a length of about 650 mm of the panel between the top (50 mm) and bottom (50 mm) stiffened regions. Also, separation of the four stringers from the panel happened as an onset of fracture during testing without fiber breakage.

Finite Element Analysis

The finite element analysis is carried out using a four-node bilinear plate/shell element with six degrees of freedom (three translations and three rotations). Beam elements are considered to incorporate the aluminum sections used on both ends of the panel. Geometric nonlinear analysis is carried out with a load increment of 400 kg up to 3000 kg, beyond which it is reduced to 100 kg. Analysis is also carried out with an increment of 50 kg instead of 100 kg toward the failure load to obtain a more accurate failure load. The model for delamination analysis differs slightly from the model used for static compression and buckling.

For the evaluation of the strain energy release rate, delamination is introduced in the middle of the panel between each stringer and the base panel. The length of the delamination varied from 1 to 22.5 mm. The stiffener and the panel are modeled as two separate structures in the regions of delamination. At the end of delamination where a perfect bond between the panel and stringer exists, common nodes are used. The strain energy release rates for the opening mode G_{I} and shear mode G_{II} are evaluated using the well-known formulas based on the virtual crack closure technique.[8] These values are calculated for all of the plate elements forming the delamination at the eight regions (on each stringer there are two base flanges) idealized by 16 elements, and the average values are computed from the analysis. The finite element model was refined at these regions, and convergence was established. Hence in the present study the relatively coarse mesh is used. Now by comparing the total strain energy release rate ($G = G_{\mathrm{I}} + G_{\mathrm{II}}$) value with the delamination fracture toughness value, the load at which delamination fracture occurs can be estimated.

Boundary Condition

A fixed boundary condition is given at the top and bottom edges of the panel but for load direction at the bottom (Fig. 1). The two lateral edges are free. Compressive loads are applied as point loads at the bottom nodes on the beam elements that represent the T section (which passes through the slit for the full width of the panel) along the stringer direction (along 750-mm height) (Fig. 1).

Results and Discussion

Based on the analyses following the Tsai–Wu failure criterion, the compressive load is calculated to be 58.72 kN, and the critical buckling load is 47.09 kN. The test showed a delamination mode of fracture by which stringers separated from the panel at 46.75 kN without fiber breakage.

A geometric nonlinear analysis is carried out in 10 increments up to a load of around 45 kN. Calculated maximum strains are compared with test at three locations (middle and 70 mm from top and bottom; Fig. 1) at the three midbays of the base panel (same side of the stiffener) and three other locations behind the stiffener obtained from the test. More details of test data on strains and their comparison with analysis results are available in Ref. 9. Comparison of strains from the test and nonlinear analysis are shown in Figs. 2–4. Up to about 65% of failure load, a good agreement is noted between the test and analysis. The test data showed a nonlinearity of 6.9 to 18.3% on the measured fiber strains at locations that are on the same side of the stiffener and 19 to 32% behind the stiffener side. To achieve good agreement between the test and analysis, the load increment beyond around 30 kN is reduced from 4 to 1 kN. However, toward the failure load to obtain convergence for the solution, load increment is further reduced to 0.5 kN. The discrepancy between the test data and analysis might be caused by the load increment considered in the analysis. It is quite obvious that at the point of failure instability

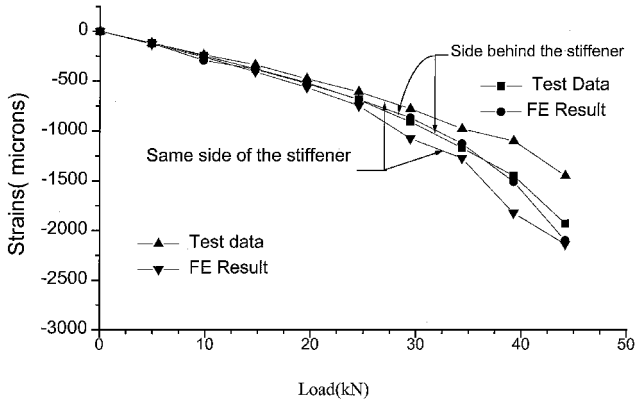

Fig. 2 Variation of strain with load in the midbay (right side) of the base panel.

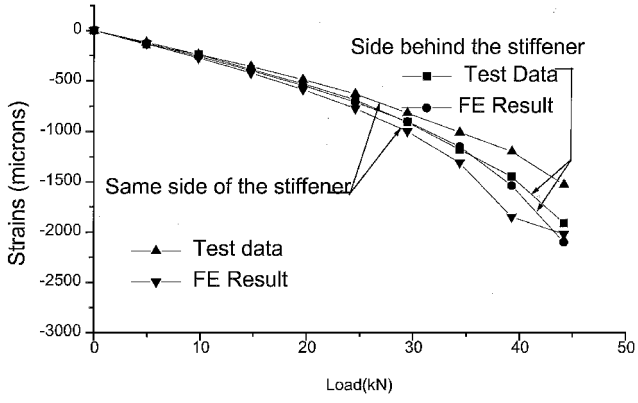

Fig. 3 Variation of strain with load in the midbay (middle) of the base panel (Fig. 1).

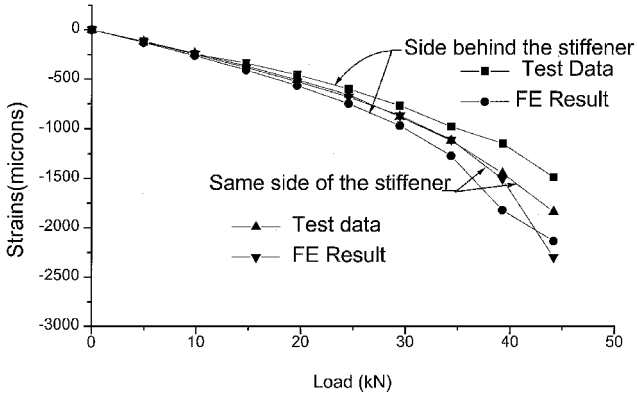

Fig. 4 Variation of strain with load in the midbay (left side) of the base panel.

occurs. In other words, the solution might not converge. This is also one of the approximate methods of determining failure load from analysis.

Mode I and mode II strain energy release rates G_{I} and G_{II} are calculated for different delamination lengths, which are varied from 1 to 22.5 mm and are shown in Fig. 5. Critical opening and shear modes strain energy release rates G_{Ic} and G_{IIc} (Ref. 7) values are 60 and 240 J/m,^{2} respectively. The total critical strain energy release rate G_c is the sum of G_{Ic} and G_{IIc} for a given mode ratio of G_{II}/G_c (Ref. 7). The variation of G_{II} and G_{I} with respect to delamination lengths is shown in Fig. 5. Because in this case the value of G_{I} is very small, only G_{II} is taken for determining the failure load caused by delamination growth.

From Fig. 5 the value of G_{II} corresponding to zero delamination length is estimated by extrapolating the curve to meet the Y axis. This value of G_{II} is found to be 40 J/m^2, corresponding to a zero delamination length. The delamination fracture load is estimated as 48.9 kN ($240^{1/2} \times 20/40^{1/2}$ for an axial load of 20 kN).

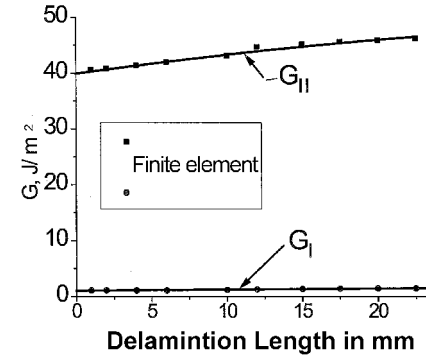

Fig. 5 Variation of G_{I} and G_{II} with delamination length.

Delamination occured between +30 deg of the skin and +45 deg of the stringer. The delamination fracture toughness was measured for 0-deg (Ref. 7) laminate.

Conclusions

A stringer stiffened composite panel has been tested under axial compression until failure, and the mode of failure has been observed as an onset of fracture resulting in making the separation of the stringer happen from the base panel at 46.75 kN. A good agreement in the fiber strains of the base panel at six locations obtained by the geometric nonlinear finite element analysis has been observed with the test data. The delamination fracture load is evaluated as 48.9 kN based on the strain energy release rate approach. An independent assessment by finite element analysis gives the buckling load as 47.09 kN. Taking into account 5–10% error in the testing, it has been concluded that the delamination fracture follows buckling.

Acknowledgment

The authors express their sincere gratitude toward S. Sridhar, Engineer, Composite Structures Division, Composite Material System Group, Vikram Sarabhai Space Center, Thiruvananthapuram, India, for fabrication and testing of the composite panel, without which the work would not be completed.

References

[1]Gotsis, P. K., and Chamis, C. C., "Effect of Combined Loads on Durability of a Stiffened Adhesively Bonded Composite Structure," *Proceedings of the 36th AIAA/ASME/ASCE/AHS/ASC Structures, Structural Dynamics, and Materials Conference*, AIAA, Washington, DC, 1995, pp. 1083–1092.

[2]Chamis, C. C., and Gotsis, P. K., "Damage Tolerance of Composite Pressurized Shells," *Proceedings of the 37th AIAA/ASME/ASCE/AHS/ASC Structures, Structural Dynamics, and Materials Conference*, AIAA, Reston, VA, 1996, pp. 2112–2121.

[3]Minnetyan, L., and Rivers, J. M., "Damage Progression in Stiffened Composite Panels," *Proceedings of the 36th AIAA/ASME/ASCE/AHS/ASC Structures, Structural Dynamics, and Materials Conference*, AIAA, Washington, DC, 1993, pp. 436–444.

[4]Starnes, J. H., Knight, N. F., and Rouse, M., "Post Buckling Behaviour of Selected Flat Stiffened Graphite Epoxy Panels Loaded in Compression," *AIAA Journal*, Vol. 23, No. 8, 1985, pp. 1236–1246.

[5]Stevens, K. A., Ricci, R., and Davies, G. A., "Post Buckling Failure of Composite Compression Panels," *Proceedings of the 19th Congress of the International Council of Aeronautical Sciences*, Vol. 3, 1994, pp. 2975–2981.

[6]Sobel, L., and Sharps, D., "Comparison of Analytical and Experimental Results for the Post Buckling Behavior of a Stiffened Flat Composite Shear Panel," *Proceedings of the 35th AIAA/ASME/ASCE/AHS/ASC Structures, Structural Dynamics, and Materials Conference*, AIAA, Washington, DC, 1994, pp. 449–457.

[7]Jose, S., Kumar, R. R., Rao, G. V., and Sriram, P., "Studies on Mixed Mode Interlaminar Fracture Toughness of M55J/M18 Carbon/Epoxy Laminates," *Advanced Composites Letters*, Vol. 9, No. 5, 2000, pp. 335–340.

[8]Wang, J. T., Raju, I. S., Davila, C. G., and Sleight, D. W., "Computation of Strain Energy Rlease Rate for Skin-Stiffener Debonds Modeled with Plate Elements," *Proceedings of the 34th AIAA/ASME/ASCE/AHS/ASC Structures, Structural Dynamics, and Materials Conference*, AIAA, Washington, DC, 1993, pp. 1680–1692.

[9]Renjith, G., "Analysis and Design Modification of Compressively Loaded Stringer Stiffened Composite Panel," M.Tech. Thesis, Dept. of